

Scientific Paper

Doi: <http://dx.doi.org/10.1590/1809-4430-Eng.Agric.v43n3e20220121/2023>**ANALYSIS AND EXPERIMENTATION OF THE CRUSHING AND SEPARATION PROCESS OF THE ROOT-SAND COMPLEX OF HARVESTED AND EXCAVATED *Cyperus esculentus* L. IN DESERTS****Minghao Pei<sup>1,2</sup>, Shiguan An<sup>1,2</sup>, Shen Chen<sup>1,2</sup>, Jiangtao Qi<sup>1,2\*</sup>, Yaping Li<sup>1,2\*</sup>**

\*Corresponding author. E-mail: 510014078@qq.com | ORCID ID: <https://orcid.org/0000-0002-1622-4186> (Jiangtao Qi); E-mail: 1015883488@qq.com | ORCID ID: <https://orcid.org/0000-0001-9766-3908> (Yaping Li).

**KEYWORDS**

*Cyperus esculentus*, excavation, root-sand complex, rotary tillage, vibrating shovel.

**ABSTRACT**

The aim of this study is to simplify the difficult excavation that is caused by the root-sand complex in the process of harvesting *Cyperus esculentus* in the desert of Xinjiang by performing mechanical tests and analysis of the interaction between the vibrating excavation shovel and the rotary blade on the root-sand complex. The rotary blade number, rotary blade speed and digging depth were used as the test parameters, and the *Cyperus esculentus* breakage rate, root-grass crushing rate, and soil carrying rate were used as the test indicators. The characteristics of the influence of various factors and their interaction on the crushing and separation of the root-sand complex were explored. A parameter combination optimization model is verified by experimental data. The test results showed that the optimal combination was as follows: the number of rotary blades was 20, the rotational speed of the rotary blade was 373 r/min, and the digging depth was 12 cm. At this time, the *Cyperus esculentus* breakage rate, root-grass crushing rate, and soil carrying rate were 2.62%, 63.68% and 55.40%, respectively. This study can support the development of a *Cyperus esculentus* harvester suitable for deserts in Xinjiang.

**INTRODUCTION**

*Cyperus esculentus* is a perennial herb of the Cyperaceae family that can be used as grain, oil and feed. This herb is an important oil crop with the characteristics of drought resistance, waterlogging resistance, barren resistance and strong adaptability (Yang, 2017; Zhang et al., 2019; Wang, 2020a). *Cyperus esculentus* can maintain and restore the ecosystem in sandstorm areas and thus increase the profitability of farming to improve people's living standards (Wang, 2022). Therefore, some desert areas in Xinjiang use oil bean as the main crop variety. *Cyperus esculentus* has been planted on a large scale in Xinjiang. For example, in Xing'an town, Tumushuke city, alone, the planting area reached more than 13 km<sup>2</sup> in 2020. Moreover, the harvesting process of *Cyperus esculentus* plants is labor intensive and expensive (Wang et al., 2019; Yang & Zhu, 2020; Lu et al., 2019; Huang et al., 2013), especially considering the climate characteristics of Xinjiang, which has a large temperature difference between the day and

night, extremely low precipitation and higher requirements for harvest timeliness (Jing et al., 2014). In harvesting *Cyperus esculentus*, the objects that are being handled are *Cyperus esculentus*, the roots and the sandy soil. In particular, the network-like fibrous root system of *Cyperus esculentus* is developed and intertwined with sandy soil to form a complex composite structure (hereafter referred to as the root-sand complex), which makes the binding strength of the composite higher than that of ordinary sandy soil and leads to problems such as difficulty in excavation during harvesting. In response to the above problems, this paper applied a *Cyperus esculentus* excavation device using rotary tillage technology and vibratory digging technology. The process of crushing and separating the root-sand complex of *Cyperus esculentus* was studied and tested.

Due to the characteristics of good soil cutting and strong soil breaking, rotary tillage technology has been widely used (Lin et al., 2016). In the early 1970s, Hendrick and Gill conducted a series of studies on the design

<sup>1</sup> College of Mechanical and Electrical Engineering, Shihezi University, Shihezi, Xinjiang, China.

<sup>2</sup> Engineering Research Center for Production Mechanization of Oasis Special Economic Crop, Ministry of Education, Shihezi, Xinjiang, China.

Area Editor: Renildo Luiz Mion

Received in: 7-29-2022

Accepted in: 6-14-2023

parameters and working parameters of rotary blades, which laid a theoretical foundation for research on the optimization of rotary blades (Hendrick & Gil, 1978). Using classical mechanics theory, Ahmadi et al. deduced the dynamic torque calculation model of a rotary blade. Compared with the test results completed by Chertkiattipol et al., the torque calculation result has an error of approximately 5% (Ahmadi, 2017; Chertkiattipol & Niyamapa, 2010). Matin et al. analyzed the torque, power and energy consumption characteristics of C-shaped machetes, half-width knives and straight knives at four rotational speeds and recorded the entire process of the rotary cultivator during excavation with the help of a high-speed camera (Matin et al., 2015). Marenya, Salokhe et al. studied the traction force during the working process of a rotary blade (Marenya, 2009; Salokhe & Ramalingam, 2003). Iwasaki et al. divided the rotary blade into the curved knife and the straight knife and analyzed the working resistance of each part (Iwasaki et al., 1992). Asl and Singh established the dynamic and static soil cutting resistance formulas of the rotary blade and analyzed the soil cutting energy consumption by means of computer and numerical methods (Asl & Singh, 2009). Moreover, the vibration excavation method is a common excavation method. According to the vibration form of the soil-contacting parts, this method is divided into self-excited vibration and forced vibration. Self-excited vibration does not require additional power input and is due to the change in excavation resistance exciting elastic soil-contacting components to generate vibration. The research shows that the self-excited vibration soil-contacting member has a certain drag reduction effect (Soeharson & Radite, 2010; Wang et al., 2016; Berntsen et al., 2006); the forced vibration excavation method requires external energy and a vibration mechanism to drive the soil-contacting parts to vibrate at a fixed frequency and amplitude. Many scholars have carried out related studies on the above two methods, different component structures and their application conditions (Rao

et al., 2019; Rao et al., 2018; Razzaghi & Sohrabi, 2016; Niyamapa & Salokhe, 2000; Shahgoli et al., 2010; Shahgoli et al., 2009; Koc et al., 2017), but due to the different structural types of soil-contacting components and soil working conditions, the excavation effects are different.

In summary, problems such as the difficulty of excavation due to the root-sand complex arise during the harvesting of *Cyperus esculentus* in the desert areas of Xinjiang. This paper investigates the process of crushing and separation of the *Cyperus esculentus* root-sand complex in excavation operations. The *Cyperus esculentus* root-sand complex was taken as the research objective, and crushing and separation tests were performed with a self-developed *Cyperus esculentus* digging device using rotary tillage technology and vibratory digging technology. The breakage and separation characteristics of the root-sand complexes were studied through orthogonal tests of related parameters. Through the application of the above technology and experimental research, the crushing and separation of the *Cyperus esculentus* complex was accomplished while harvesting *Cyperus esculentus* in an extremely dry desert environment. This study provides support for the development of a *Cyperus esculentus* harvester suitable for the Xinjiang desert area.

## MATERIAL AND METHODS

### Analysis of the breakage and separation process of the root-sand complex

#### Analysis of the rotary blade operation process

When the rotary blade is working, it will cut and throw the sand and the root-sand complex. The tangential surface of the blade enters the soil and compresses and deforms the sand to form a shear plane. Then, the blade forms a soil ridge, part of which slides down to both sides of the tool, with the remainder sliding along the tangential surface. The force analysis is shown in Figure 1.

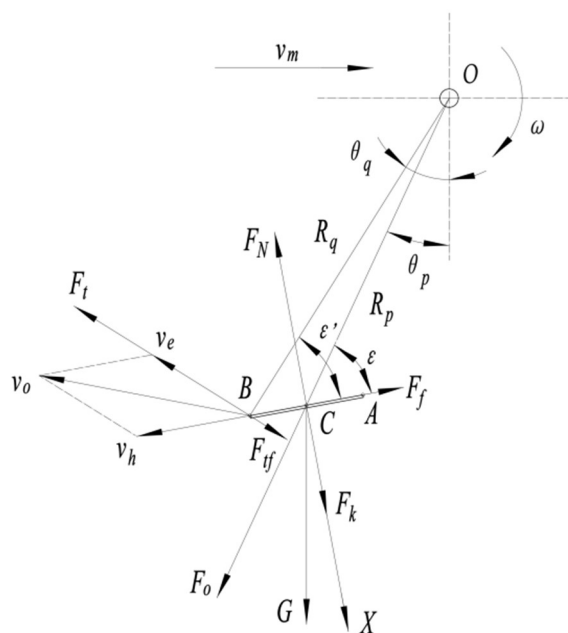


FIGURE 1. Sandy soil force analysis schematic. Notably,  $O$  is the rotation center of the rotary blade shaft,  $R_q$  is the outer radius of the tangent,  $AB$  is the tangential plane of the rotary blade,  $\varepsilon'$  is the tangent front inclination angle,  $R_p$  is the distance from the simplified centerpoint  $C$  of the force to the center of rotation when the sand is thrown on the tangent surface,  $\varepsilon$  is the angle between  $R_q$  and the tangent plane,  $\omega$  is the rotary blade speed,  $\theta_p$  is the angle that  $R_p$  has turned from the vertical position, and  $\theta_q$  is the angle that  $R_q$  has turned from the vertical position. Simplified calculations are performed here without considering the tangential surface effects.

When the rotary blade is working (the force analysis is shown in Figure 1), in addition to cutting and throwing sand and soil, the blade cuts, crushes and throws the *Cyperus esculentus* root-sand complex. For the rotary blade to effectively cut sand and root-sand complexes, satisfying [eq. (1)] is necessary:

$$\begin{cases} \frac{F_T - Ft_f}{M_t} > \tau_s = \tan \varphi_s + c_s \\ \frac{F_T - Ft_f}{M_t} > \tau_{gst} = \sigma \tan \varphi_{gst} + c_{gst} \end{cases} \quad (1)$$

Where:

- $F_t$  is the shear force on the material, N;
- $F_{tf}$  is the shear resistance of the material, N;
- $M_t$  is the shearing surface area of the rotary blade, mm<sup>2</sup>;
- $\tau_s$  is the shear strength of sand, Pa;
- $\tau_{gst}$  is the shear strength of the *Cyperus esculentus* root-sand complex, Pa;
- $\sigma$  is the normal stress during shearing, Pa;
- $\varphi_s$  is the internal friction angle of sand;
- $\varphi_{gst}$  is the internal friction angle of the root-sand complex;
- $c_s$  is the cohesion of sand, Pa, and
- $c_{gst}$  is the cohesion of the root-sand complex, Pa.

Due to the special physical properties of sand, its cohesion can be ignored here. The cohesion  $c$  of the *Cyperus esculentus* root-sand complex of oleifera can be selected as 10~20 kPa with reference to the complex characteristics of other plants (Yan et al., 2022; Yang et al., 2021; Wang, 2020b). Due to the constant shearing surface area of the rotary blade during work, according to [eq. (1)], the size of the shear force is the main factor that affects the cutting operation. In actual work, the rotational speed of the rotary cutter shaft determines the magnitude of the shear force, so the rotational speed of the rotary cutter shaft will affect the cutting operation of the root-sand complex.

At the same time, during the throwing operation, to avoid generating friction so that the sand and the root-sand complex can be thrown out, the resultant force perpendicular to the tangential plane on the material must be less than 0 (consider the action of centrifugal force  $F_o$ ); that is,

$$\sum F(X) < 0 \quad (2)$$

The following equations can be obtained from [eq. (2)] and Figure 1:

$$\begin{aligned} \sum F(X) &= mg \sin(\theta_p + \varepsilon) + F_o \sin \varepsilon + aM_Y + F_k \\ \sum F(X) &= mg \sin(\theta_p + \varepsilon) + m\omega^2 R_p \sin \varepsilon + aM_Y + 2m\omega v_h \end{aligned} \quad (3)$$

Where:

$\sum F(X)$  is the resultant force perpendicular to the tangential plane on the material, N;

$m$  is the material quality, g;

$g$  is the acceleration of gravity, m·s<sup>-2</sup>;

$a$  is the adhesion factor;

$M_Y$  is the leaf area, mm<sup>2</sup>;

$F_o$  is the centrifugal force of the material, N;

$F_k$  is the inertial force of the material, N, and

$v_h$  is the relative velocity of the material moving along the tangential plane (as shown in Figure 3,  $v_e$  is the implicated velocity of the material moving along the tangential plane, and  $v_o$  is the absolute velocity of the material moving along the tangential plane).

Equation (3) can be substituted into [eq. (2)]. Since the adhesion factor of sand is small, the  $aM_Y$  term is ignored. At the same time, because the rotating speed of the rotary blade is fast, the relative motion of the material along the tangential plane is not currently considered; thus, the  $F_k$  term is ignored. Then, the following formula can be obtained:

$$n_m > \frac{30}{\pi} \sqrt{\frac{g \sin(\theta_p + \varepsilon)}{R_p - \sin \varepsilon}} \quad (4)$$

From [eq. (4)], when the rotary blade rotates so that the tangential plane is in a horizontal position, materials such as sand and soil are most likely to leave the tangential plane. In addition, in the independent construction of the *Cyperus esculentus* excavation device when the rotary tillage blade IT245 is selected, in the calculation that  $R_p = 245$  mm,  $\varepsilon = 80^\circ$ ; at this time, only when the rotary tillage blade speed  $n_m > 61$  r/min can the throwing operation be complete. During the excavation process, the rotation speed of the rotary blade will affect the number of materials that are cut and the time to cut those materials, which in turn affects the amount and magnitude of the force on the material. Through the calculation and analysis of Eq. (1) and (4), the magnitude of the relevant force will lead to changes in the degree of cutting and the degree of fragmentation of *Cyperus esculentus* and the root-sand complex. At the same time, the rotation speed of the rotary cultivator will affect the difference in the throwing position and the initial velocity of the throwing. According to the traditional rotary blade motion analysis, the number of rotary blades will also affect the number of times the material is cut, which will lead to changes in the degree of fragmentation of *Cyperus esculentus* and the root-sand complex.

### Analysis of the vibration excavation process

During vibration excavation, the digging resistance and vibration resistance of the device will affect the magnitude of the force on the material. Thus, in the process of analyzing the vibration digging shovel, the influence of the resistance should be considered. According to the force of the vibrating excavation shovel during excavation and the force of the excavated sand, the vibration excavation shovel is divided into the vibrating excavation flat shovel and the vibrating grid screen for analysis (Figure 2)

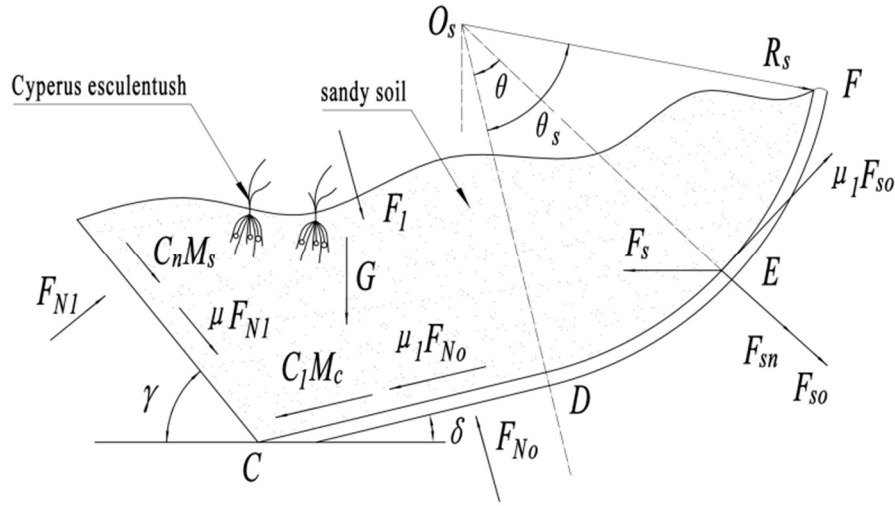


FIGURE 2. Vibration excavation process force analysis schematic. Notably,  $CD$  is the vibrating digging plane shovel surface;  $DF$  is the arc-shaped vibrating grid screen (the cross section is circular);  $E$  is a point on the arc sieve;  $G$  is the gravity of sandy soil on the shovel surface;  $C_n$  is the cohesion factor of sandy soil;  $C_1$  is the sand adhesion factor;  $F_1$  is the acceleration force of the sandy soil moving along the shovel surface;  $F_{Nl}$  is the normal load on the front failure surface;  $F_{No}$  is the normal load of the shovel surface on the sandy soil;  $M_s$  is the shear area within the sandy soil;  $M_c$  is the area of the digging shovel;  $\gamma$  is the inclination angle of the front failure surface;  $\delta$  is the tilt angle of the shovel surface;  $\mu$  is the internal friction factor of the sandy soil;  $\mu_1$  is the friction factor between the sandy soil and the excavation shovel;  $O_s$  is the center of the arc sieve circle;  $F_s$  is the arc screen traction force;  $F_{s0}$  is the sticky resistance caused by the sandy soil to the arc sieve;  $F_{sn}$  is the normal positive pressure on the curved screen;  $R_s$  is the radius of the curved screen;  $\theta_s$  is the angle of the  $DF$  section arc screen; and  $\theta$  is the angle of deflection of a point  $E$  on the curved sieve.

Moreover, the resistance calculation formula of the vibration excavation plane shovel is as follows:

$$\begin{cases} w_{cc} = \frac{G}{Z_c} + \frac{C_n M_s + F_1}{Z_c (\sin \gamma + \mu \cos \gamma)} + \frac{C_1 M_c}{Z_c (\sin \delta + \mu_1 \cos \delta)} \\ w_{ct} = (C_n M_s + \mu F_{Nl}) \sin \gamma + (C_1 M_c + \mu_1 F_{No}) \sin \delta + F_1 \cos \delta + G \end{cases} \quad (5)$$

Where:

$w_{cc}$  is the horizontal resistance of the vibratory digging shovel;

$w_{ct}$  is the vertical resistance of the vibratory digging shovel, and

$Z_c$  is a constant.

The viscous drag principle can be applied in the force analysis of the vibrating grizzly screen. Meanwhile, to simplify the calculation, the vertical height of arc  $DF$  is approximated to be equal to the digging depth  $d$ . The formula for calculating the resistance of a vibrating grizzly screen can be obtained as follows:

$$\begin{cases} w_{sc} = \int_0^{\delta - \arccos\left(\frac{R_s \cos \delta - d}{R_s}\right)} \left[ \frac{F_{sn} + Z_s (6\pi\eta v_m r_0)}{\sin(\delta + \theta)} + \frac{\mu_1 F_{sn}}{\cos(\delta + \theta)} \right] d\theta \\ w_{st} = \int_0^{\delta - \arccos\left(\frac{R_s \cos \delta - d}{R_s}\right)} \left[ \frac{F_{sn} + Z_s (6\pi\eta v_m r_0)}{\cos(\delta + \theta)} + \frac{\mu_1 F_{sn}}{\sin(\delta + \theta)} \right] d\theta \end{cases} \quad (6)$$

Where:

$w_{sc}$  is the horizontal resistance of the vibrating grizzly screen;

$w_{st}$  is the vertical resistance of the vibrating grizzly screen;

$\eta$  is the viscosity coefficient of the sandy soil;

$v_m$  is the forward speed of the device;

$r_0$  is the radius of the circular cross section of the curved vibrating grizzly screen, and

$Z_s$  is a constant.

The digging depth will first affect the sand quality on the shovel surface, which will affect the normal positive pressure on each area. According to the analysis of Figure 2, eqs (5) and (6), in addition to the physical properties of the sand and root-sand complex, the main factors that affect the stress of the sand and the root-sand complex are the digging depth and the inclination of the screen surface.

The inclination of the screen surface will mainly affect the positive pressure of the material and the forward resistance of the device. This paper focuses on the process of fragmentation and separation of the *Cyperus esculentus* root-sand complex at harvest. The inclination of the screen surface was not a major influence in this process, so the inclination of the screen surface was not considered an influencing factor in the subsequent tests. Due to the relatively fixed growth depth of *Cyperus esculentus* and the physical characteristics of sandy soil, the digging depth influences the action of the relevant forces on the material and the cutting position of the rotary blade. Excessive digging depth will prevent the rotary blade from cutting the material and affect the crushing and separation of the root-sand complex. A digging depth that is too small will lead to inadequate cutting of the material, which affects the vibration separation effect of the vibratory excavation shovel.

### Test material

The test samples were randomly selected from the *Cyperus esculentus* planting test base of the 54th Regiment of the Third Division of the Xinjiang Production and Construction Corps. The variety was Zhongyousha No. 1,

and the sampling period was October 2021. During the test, the national standard "GB/T5262-2008 General Provisions for Determination Methods of Agricultural Machinery Test Conditions" was referenced. A square box of 1 m<sup>2</sup> was used to select 1 m<sup>2</sup> of *Cyperus esculentus* in the field test area for harvesting *Cyperus esculentus*, and 1 m<sup>2</sup> of *Cyperus esculentus* plant and grain samples of *Cyperus esculentus* were collected according to the cutting height.

Measurements, calculations and statistical tests of the characteristic parameters of *Cyperus esculentus* are shown in Table 1. At the same time, the following characteristic parameters of sandy soil in the same experimental area were measured: the density was 1.638 g·cm<sup>-3</sup>; the surface moisture content was 2.59%; and the average moisture content of the sand that was entrained by the root-sand complex was 6.51%.

TABLE 1. Table of *Cyperus esculentus* characteristic parameters for testing.

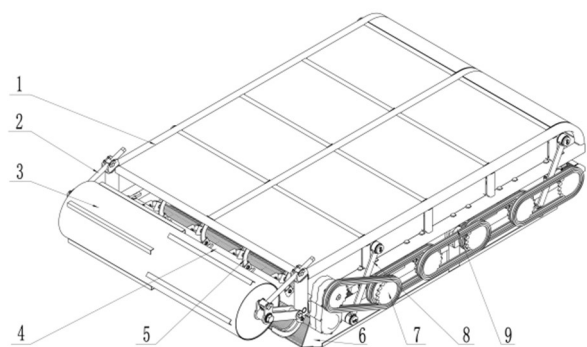
Name	Parameter
Cyperus esculentus plant quantity of 1 m <sup>2</sup> (g)	1582
Cyperus esculentus yield of 1 m <sup>2</sup> (g)	664
Cyperus esculentus grass and root quantity of 1 m <sup>2</sup> (g)	918
Yield (kg·km <sup>-2</sup> )	996.51
Cyperus esculentus grass to grain ratio	1.38
Cyperus esculentus moisture content of grain/%	25~40
Hundred grain mass (g)	104.33
The root depth (cm)	10.88
Cyperus esculentus growth depth (cm)	6.73
Plant stubble height (cm)	8.44
Cyperus esculentus grain size (mm)	8~12

**Test equipment**

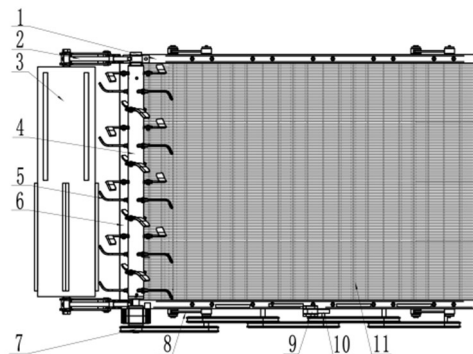
The test equipment mainly included a self-built oil bean digging device, a 101-IB type electric heating blast constant temperature drying oven, an electronic scale JM-B5003 (range: 0~500 g, graduation value: 0.001 g), an electronic scale JSB15-05 (range: 0~15 kg, graduation value: 0.5 g), a 20 m tape measure, a Vernier caliper, scissors, and receiving bags.

The *Cyperus esculentus* excavation device mainly includes a frame, a depth-limiting wheel component, a

rotary blade part and a vibration excavation part. The height of the depth-limiting wheel is controlled by a pair of rotating lead screws. The components of the rotary blade part use a detachable rotary blade to change the number of rotary blades. In addition, the shaft of the rotary blade is driven by a set of sprockets. During operation, the rotational speed of the rotary blade shaft is changed by changing the speed of the engine and the number of teeth in the sprocket at the end of the sprocket group. As a result, the vibration frequency of the vibrating shovel is guaranteed. A schematic diagram of the structure is shown in Figure 3.



(a) Top view of complete machine



(b) Axis side view of complete machine (without the top cover of the rack)

FIGURE 3. Structural diagram of the *Cyperus esculentus* digging device. 1. Frame assembly; 2. Regulator of depth-limiting wheel; 3. Depth-limiting wheel; 4. Rotary tillage cutter shaft; 5. Rotary cutter; 6. Vibratory digging shovel; 7. Sprocket assembly; 8. Connecting rods of vibratory digging shovel; 9. Rollers; 10. Cam

The working principle of the *Cyperus esculentus* excavation device during the excavation operation is as follows: the harvester rotates the excavating device down, and the depth-limiting wheel contacts the ground to provide support at the front end, which limits the digging depth; the harvester transmits power to the vibration excavation part and the rotary blade part in turn through the sprocket; at the same time, the cam is driven to vibrate the vibrating digging part by hitting the roller that is connected to the vibrating screen; finally, the rotation of the sprocket will also drive the rotary blade to rotate and start the rotary tillage operation.

## Experimental method

### *Cyperus esculentus* excavation test

Before the test, the catch bag was attached to the back end of the excavation device to collect excavation samples for each set of tests. Prior to the relevant trials, a review of relevant references and standards did not reveal any harvesting standards that met the criteria for *Cyperus*

*esculentus*. Therefore, the general standard for harvesters, "GB/T 8097-2008 Equipment for harvesting-Combine harvesters-Test procedure", as well as the harvesting standards for crops similar to *Cyperus esculentus*, "JB/T 11912-2014 Soybean combine harvester" and "NY/T 502-2016 Operating quality for peanut harvesters," were referred to during the test. Additionally, to evaluate the degree of plant fragmentation, the standard "JB/T 8401.2-2007 Rototill combine equipment-Rototill scarifying-paring-ridging machine" is also referred to here. Furthermore, the working length of each group of tests was set to 25 m, and each group of tests was repeated 3 times. The samples were processed according to the calculation method of the experimental data, and the average value was calculated to obtain the *Cyperus esculentus* breakage rate, root-grass crushing rate, and soil carrying rate of each group of experiments. The *Cyperus esculentus* excavation tests were completed in sequence according to the test serial numbers, and the test process is shown in Figure 4.



FIGURE 4. Test process.

### Test index calculation method

The mass of all the *Cyperus esculentus*, including the mass of the *Cyperus esculentus* that is damaged by the excavation, in the samples that are taken after excavation are determined. Equation (7) is used to calculate the breakage rate of *Cyperus esculentus*.

$$P_d = \frac{m_1}{m_2} \times 100\% \quad (7)$$

Where:

$P$  is the breakage rate;

$m_1$  is the quality of the *Cyperus esculentus* that is damaged due to excavation, g, and

$m_2$  is the quality of *Cyperus esculentus*, g.

Additionally, all *Cyperus esculentus* stubble and broken grass in the samples taken after excavation are determined. The total quality of the broken grass and root stubble and the quality of the broken grass and root stubble whose length is less than or equal to 50 mm (excluding the length of fibrous roots) are determined. The root-grass crushing rate is calculated according to [eq. (8)].

$$F_g = \frac{M_h}{M_z} \times 100\% \quad (8)$$

Where:

$F_g$  is the root-grass crushing rate;

$M_h$  is the quality of the stubble and grass with length  $\leq 50$  mm, g, and

$M_z$  is the total stubble and grass quality, g.

Equation (9) is used to calculate the soil carrying rate of the root grass.

$$T = \frac{m_3}{m_4} \times 100\% \tag{9}$$

Where:

$T$  is the soil rate;

$m_3$  is the mass of the soil in the sample (*Cyperus esculentus* plant sample) that was taken after excavation, g, and

$m_4$  is the quality of the *Cyperus esculentus* plant sample, g.

## RESULTS AND DISCUSSION

### Orthogonal design of the experiments

According to the calculation method of the test index, the calculation and statistics of the breakage rate, the root-grass crushing rate and the soil carrying rate are

completed. Considering the harvesting efficiency of *Cyperus esculentus* and the width of the device used, the operating speed was 0.2 m/s, the amplitude was 9 mm, and the vibration frequency was 12.4 Hz.

Refer to the theoretical study in section 2.1 of the article. The number of rotary tillage blades, rotary tillage blade speed and digging depth are important factors that affect the quality of operation of the device and material crushing and separation. Therefore, they were chosen as test factors. Through the project team's preliminary single-factor test, it was found that at a rotary tillage blade number of 18~22, a rotary tillage blade speed of 335~405 r/min and a digging depth of 10~14 cm, the breakage rate and soil carrying rate were very low and the root-grass crushing rate was very high. Based on the parameter ranges of these test factors, the levels of the three test factors for this experiment were determined, as shown in Table 2. A total of 17 sets of experiments were carried out by using the orthogonal test method and the L(3<sup>4</sup>) orthogonal table. The design table and the statistics of the breakage rate, root-grass crushing rate and soil carrying rate are shown in Table 3.

TABLE 2. Digging parameter level.

Code	Number of rotary blades	Rotary blade speed (r/min)	Digging depth (cm)
-1	18	335	10
0	20	370	12
1	22	405	14

TABLE 3. Experimental layout and results.

Code	Number of rotary blades <i>A</i>	Rotary blade speed <i>B</i>	Digging depth <i>C</i>	Breakage rate $P_d$ /%	Root-grass crushing rate $F_g$ /%	Soil carrying rate $T$ /%
1	-1	-1	0	3.73	28.51	73.62
2	1	-1	0	4.97	55.00	163.7
3	-1	1	0	4.47	45.51	74.08
4	1	1	0	5.50	54.43	79.67
5	-1	0	-1	5.68	38.83	65.16
6	1	0	-1	7.57	58.33	94.44
7	-1	0	1	4.86	44.39	73.90
8	1	0	1	5.46	51.40	123.87
9	0	-1	-1	4.71	38.13	116.67
10	0	1	-1	8.46	25.87	71.92
11	0	-1	1	4.29	34.11	119.98
12	0	1	1	3.48	52.45	124.27
13	0	0	0	2.45	58.72	70.35
14	0	0	0	3.22	63.60	44.49
15	0	0	0	1.84	73.97	52.74
16	0	0	0	3.34	70.40	66.19
17	0	0	0	2.51	60.88	63.81

### Establishment of the significance test of the breakage rate regression model

According to the analysis of the test data in Table 3 and the multiple regression fitting, the analysis of variance was performed on the breakage rate, and the results are shown in Table 4.

Table 4 shows that the primary and secondary order of the influence of each factor and the interaction between the factors on the breakage rate  $P_d$  are  $C^2$ ,  $C$ ,  $A^2$ ,  $BC$ ,  $A$ ,  $B$ ,

$B^2$ ,  $AC$ , and  $AB$ . Among them,  $C^2$ ,  $C$ ,  $A^2$  and  $BC$  have a very significant influence on the breakage rate  $P_d$  ( $P < 0.01$ ), while  $A$ ,  $B$  and  $B^2$  have a significant impact on the breakage rate  $P_d$  ( $0.01 < P < 0.05$ ). After incorporating the regression sum of the squares and degrees of freedom of some insignificant interaction terms into the residual term, the analysis of the variance was performed, as shown in Table 4. The regression equation  $P_i$  of each factor on the breakage rate  $P_d$  was obtained as follows:

$$P_1 = 2.67 + 0.60A + 0.53B - 1.04C - 1.14BC + 1.33A^2 + 0.67B^2 + 1.89C^2 \tag{10}$$

TABLE 4. Analysis of the variance of the breakage rate.

Source	Sum of squares	df	Mean square	F value	P value	Significance
Model	46.08/45.66	9/7	5.12/6.52	13.62/19.19	0.0012/<0.0001	significant
A	2.83	1	2.83	7.53/8.33	0.0287/0.0180	*
B	2.22	1	2.22	5.89/6.52	0.0456/0.0310	*
C	8.67	1	8.67	23.07/25.52	0.0020/0.0007	**
AB	0.011	1	0.011	0.029	0.8689	
AC	0.42	1	0.42	1.11	0.3278	
BC	5.20	1	5.20	13.83/15.30	0.0075/0.0036	**
A <sup>2</sup>	7.41	1	7.41	19.71/21.80	0.0030/0.0012	**
B <sup>2</sup>	1.88	1	1.88	5.01/5.55	0.0602/0.0430	*
C <sup>2</sup>	15.10	1	15.10	40.18/44.44	0.0004/<0.0001	**
Residual	2.63/3.06	7/9	0.38/0.34			
Lack of fit	1.12/1.54	3/5	0.37/0.31	0.98/0.82	0.4846/0.5946	not significant
Pure Error	1.51	4	0.38			
Cor Total	48.72	16				
R <sup>2</sup>	0.9460/0.9372					

Note: The value following the slash is the result of removing the nonsignificant factors. \* means significant (0.01<P<0.05), and \*\* means very significant (P<0.01)

**Establishment of the significance test of the root-grass crushing rate regression model**

According to the analysis of the test data in Table 3 and the multiple regression fitting, the analysis of the variance was performed on the root-grass crushing rate, and the results are shown in Table 5. Table 5 shows that the primary and secondary orders of the influence of each factor and the interaction between the factors on the root-grass crushing rate  $F_g$  are B<sup>2</sup>, A, C<sup>2</sup>, BC, A<sup>2</sup>, AB, B, C, and AC.

Among them, B<sup>2</sup>, A and C<sup>2</sup> have a very significant influence on the root-grass crushing rate  $F_g$  (P < 0.01), while BC has a significant impact on the root-grass crushing rate  $F_g$  (0.01 < P < 0.05). After incorporating the regression sum of the squares and degrees of freedom of some insignificant interaction terms into the residual term, the analysis of the variance was performed, as shown in Table 5. The regression equation P<sub>2</sub> of each factor on the root-grass crushing rate  $F_g$  was obtained as follows:

$$P_2 = 63.61 + 7.74A + 2.81B + 2.65C + 7.65BC - 15.36B^2 - 12.99C^2 \tag{11}$$

TABLE 5. Analysis of variance of the root-grass crushing rate.

Source	Sum of squares	df	Mean square	F value	P value	Significance
Model	2843.19/2640.72	9/6	315.91/440.12	8.46/9.49	0.0051/0.0012	significant
A	479.26	1	479.26	12.83/10.33	0.0090/0.0093	**
B	63.34	1	63.34	1.70/1.37	0.2341/0.2698	
C	56.13	1	56.13	1.50/1.21	0.2600/0.6972	
AB	77.18	1	77.18	2.07	0.1928	
AC	39.00	1	39.00	1.04	0.3409	
BC	234.09	1	234.09	6.27/5.04	0.0408/0.0485	*
A <sup>2</sup>	86.29	1	86.29	2.31	0.1724	
B <sup>2</sup>	963.16/996.51	1	963.16/996.51	25.78/21.48	0.0014/0.0009	**
C <sup>2</sup>	684.42/712.21	1	684.42/712.21	18.32/15.35	0.0037/0.0029	**
Residual	261.54/464.01	7/10	37.36/46.40			
Lack of fit	94.87/297.34	3/6	31.62/49.56	0.76/1.19	0.5727/0.4533	not significant
Pure Error	166.67	4	41.67			
Cor Total	3104.73	16				
R <sup>2</sup>	0.9158/0.8505					

**Establishment of the significance test of the soil carrying rate regression model**

According to the analysis of the test data in Table 3 and the multiple regression fitting, the analysis of the variance was performed on the root-grass crushing rate, and the results are shown in Table 6. Table 6 shows that the primary and secondary order of the influence of each factor and the interaction between the factors on the soil carrying rate  $T$  are  $A$ ,  $B^2$ ,  $B$ ,  $AB$ ,  $C^2$ ,  $C$ ,  $BC$ ,  $A^2$ , and  $AC$ . Among

them,  $A$ ,  $B^2$ ,  $B$ ,  $AB$  and  $C^2$  have a very significant influence on the soil carrying rate  $T$  ( $P < 0.01$ ), while  $C$  has a significant impact on the soil carrying rate  $T$  ( $0.01 < P < 0.05$ ). After incorporating the regression sum of the squares and degrees of freedom of some insignificant interaction terms into the residual term, the analysis of the variance was performed, as shown in Table 6. The regression equation  $P_3$  of each factor on the soil carrying rate  $T$  was obtained as follows:

$$P_3 = 59.52 + 21.87A - 15.50B + 11.73C - 21.12AB + 12.26BC + 9.69A^2 + 28.56B^2 + 20.13C^2 \tag{12}$$

TABLE 6. Analysis of the variance of the soil carrying rate.

Source	Sum of squares	df	Mean square	F value	P value	Significance
Model	15402.97/15295.95	9/8	1711.44/1911.99	15.84/17.72	0.0007/0.0003	significant
$A$	3824.63	1	3824.63	35.40/35.44	0.0006/0.0003	**
$B$	1922.93	1	1922.93	17.80/17.82	0.0039/0.0029	**
$C$	1100.51	1	1100.51	10.19/10.20	0.0152/0.0127	*
$AB$	1784.64	1	1784.64	16.52/16.54	0.0048/0.0036	**
$AC$	107.02	1	107.02	0.99	0.3528	
$BC$	601.23	1	601.23	5.56/5.57	0.0504/0.0459	*
$A^2$	395.52	1	395.52	3.66/3.67	0.0973/0.0919	
$B^2$	3434.29	1	3434.29	31.79/31.82	0.0008/0.005	**
$C^2$	1706.94	1	1706.94	15.80/15.82	0.0054/0.0041	**
Residual	756.30/863.32	7/8	108.04/107.91			
Lack of fit	304.25/411.27	3/4	101.41/102.82	0.90/0.91	0.5161/0.5354	not significant
Pure Error	452.05	4	113.01/113.01			
Cor Total	16159.27	16				
$R^2$	0.9532/0.9466					

**Response surface analysis**

The experimental data were processed by Design-Expert 8.0.6 statistical software. The response surfaces of the significant and relatively significant interactions among the rotary blade number  $A$ , the rotary blade speed  $B$ , and the digging depth  $C$  on the breakage rate, root-grass crushing rate and soil carrying rate were obtained as shown in Figure 5.

Figure 5a shows that when the digging depth of the device is constant, the breakage rate first decreases and then increases with an increasing number of rotary blades  $A$ . The optimal number of rotary blades is 19~20. The breakage rate initially decreases and then increases with increasing rotary blade speed  $B$ . The optimal rotary blade speed is 335~384 r/min. When the number of rotary blades and the rotary blade speed are low, the rotary cultivator fails to fully throw out the material, and the number of times that the material is acted on by the rotary blade increases, which results in an increasing breakage rate  $P_d$ . However, when the number of rotating blades and rotating blade speed of the equipment are high, the force between the rotating blades and the material increases and becomes larger, which will also lead to an increase in the breakage rate  $P_d$ .

As shown in Figure 5b, when the number of rotary blades is 20, the root-grass crushing rate first increases and then decreases with an increasing rotary blade rotation speed and an increasing digging depth. The optimal rotary

blade speed is 356~384 r/min because when the rotating speed of the rotary cultivator is low, the rotary blades cannot fully cut the material, which results in a reduction in the root-grass crushing rate  $F_g$ . When the rotating speed of the rotary blades of the device is high, the throwing effect of the rotary blades increases, which also leads to a decreasing root-grass crushing rate. Currently, when the digging depth is shallow, the rotary blade cannot completely cut the roots and grass, which results in a reduction in the root-grass crushing rate  $F_g$ . When the digging depth is deep, the working part of the rotary tillage blade crosses the growth range of some roots and grasses, which results in a decrease in the root-grass crushing rate  $F_g$ .

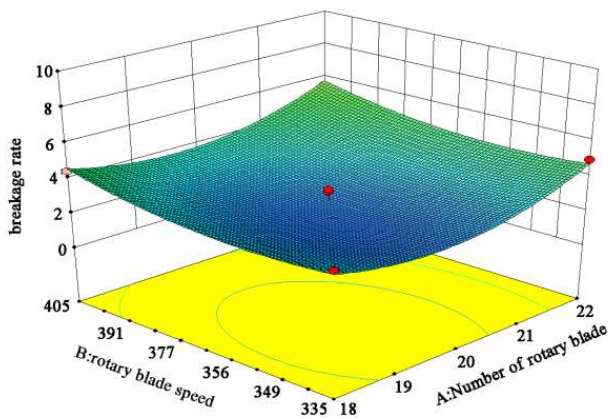
As shown in Figure 5c, when the digging depth is constant, the soil carrying rate  $T$  increases with an increasing number of rotary blades. The optimal number of rotary blades is 18~20 because the higher the number of rotary blades is, the greater the throwing action of the rotary blades. Thus, some root-sand complexes cannot be broken up, which results in an increasing soil carrying rate  $T$ . As shown in Figure 5d, when the number of rotary blades is 20, the soil carrying rate  $T$  first decreases and then increases with an increasing rotary blade speed  $B$ . The optimal rotary blade speed is 342~391 r/min because when the rotating speed of the rotary blade is low, the cutting action of the rotary blade decreases, the vibration decreases, and the root-sand complex cannot be effectively destroyed. When the

rotational speed of the rotary blade of the device is high, the throwing effect of the rotary blade increases, and the root-sand complex cannot be effectively cut, which leads to an increasing soil carrying rate. Currently, the soil carrying rate  $T$  increases with an increasing digging depth  $C$ . The optimal digging depth is 10~12 cm because the increase in the digging depth reduces the direct effect of the rotary blade on the root-sand complex, which results in an increased soil carrying rate.

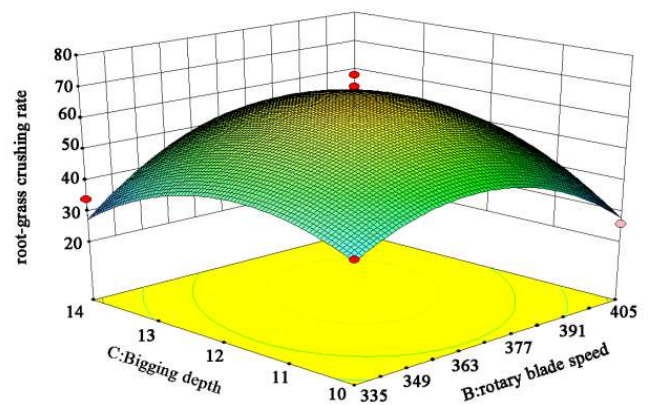
To obtain the best operating parameters, optimizing the working parameters and achieving a reasonable matching of parameters between factors are key. The objective is to have the lowest breakage rate and soil carrying rate and the highest root-grass crushing rate. The objective function and constraints are shown in [eq. (13)].

$$\begin{cases} \min P_1 \\ \max P_2 \\ \min P_3 \\ 18 \leq A \leq 22 \\ 335 \leq B \leq 405 \\ 10 \leq C \leq 14 \end{cases} \quad (13)$$

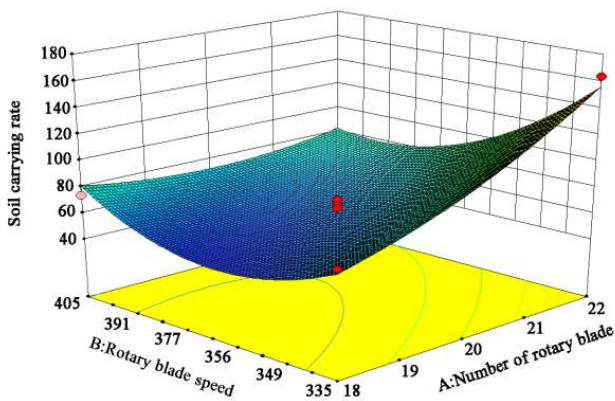
According to the actual working conditions and the abovementioned related model analysis, the solution result is as follows: the number of rotary blades is 19.74, the rotary blade speed is 372.92 r/min, and the digging depth is 12.19 cm. Currently, the breakage rate of the device is 2.58%, the root-grass crushing rate is 62.92%, and the soil carrying rate is 57.35%.



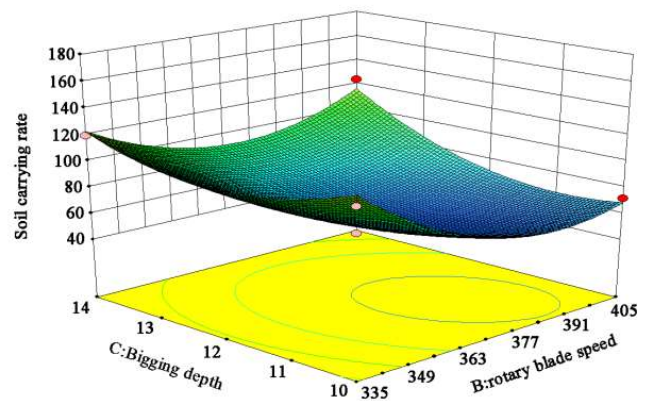
(a) Digging depth = 12 cm: breakage rate



(b) Number of rotary blades = 20: root-grass crushing rate



(c) Digging depth = 12 cm: soil carrying rate



(d) Number of rotary blades = 20: soil carrying rate

FIGURE 5. Response surface diagram of the oil bean digging device.

### Experimental verification of the optimal excavation parameter combination for the *Cyperus esculentus* excavation device

To verify the reliability of the optimization model for the combination of parameters of the *Cyperus esculentus* excavator, a validation test of the excavator was conducted in the same *Cyperus esculentus* test area based on the solved optimal combination. Considering the actual working conditions, the optimal excavation parameter combination of the *Cyperus esculentus* excavation device was adjusted to the following field verification excavation test parameter

combination: rotary blade number of 20, rotary blade speed of 373 r/min, and digging depth of 12 cm. A total of three field validation trials of the *Cyperus esculentus* excavator were completed utilizing the above combination. The mean values of the breakage rate, root-grass crushing rate and soil carrying rate were calculated for the three groups of field validation tests and were 2.62%, 63.68% and 55.40%, respectively, as shown in Table 7. Using this table and the optimization results in Section 3.2.4 to calculate the error, the breakage rate, the root-grass crushing rate and the soil carrying rate are 1.55%, 1.21% and 3.40%, respectively, with small errors.

TABLE 7. Data of the validation test for the combination of an optimum *Cyperus esculentus* digging device for harvesting.

Serial No.	Breakage rate	Root-grass crushing rate	Soil carrying rate
1	2.16	65.38	60.12
2	2.97	63.25	52.26
3	2.73	62.42	53.82
Average value	2.62	63.68	55.40

## CONCLUSIONS

(1) In view of the excavation difficulties caused by the root-sand complex during the harvesting of *Cyperus esculentus* in the Xinjiang desert area, a series of studies was conducted in this paper. A mechanical analysis of the vibrating excavation shovel and the rotary blade on the root-sand complex was carried out. The rotary blade number, rotary blade speed and digging depth were used as the test parameters, and the *Cyperus esculentus* breakage rate, root-grass crushing rate, and soil carrying rate were used as the test indicators. Thus, the trends of the various influencing factors and their interactions on the fragmentation and separation of root-sand complexes were explored.

(2) According to the principle of the response surface experimental design, the 3-factor 3-level response surface analysis method was used to conduct multifactor variance analysis on the factors that affect the experimental indicators. The results showed that the factors that affect the crushing rate of *Cyperus esculentus* were the digging depth, the rotary blade number, and the rotary blade speed, in descending order. The main factor that affected the root-grass crushing rate was the number of rotary blades. The factors that affect the root-grass carry rate were the rotary blade number, rotary blade speed, and digging depth, in descending order.

(3) The regression model was optimally solved using the optimization module in Design-Expert 8.0.6 software and experimentally verified. The test results show that the optimal combination of excavation parameters is a rotary blade number of 20, a rotary blade speed of 373 r/min, and a digging depth of 12 cm. Moreover, the breakage rate, root-grass crushing rate and soil carrying rate were 2.62%, 63.68% and 55.40%, respectively. Thus, this paper provides support for the development of a *Cyperus esculentus* harvester applicable to the desert region of Xinjiang.

**Funding:** The work was supported by China's Central Government Guides Local Science and Technology Development Fund Projects (No. 2060404).

## REFERENCES

Ahmadi I (2017) A torque calculator for rotary blade using the laws of classical mechanics. *Soil and Tillage Research* 165(1): 137-143.

Asl JH, Singh S (2009) Optimization and evaluation of rotary blade blades: Computer solution of mathematical relations. *Soil & Tillage Research* 106(106):1-7.

Berntsen R, Berre B, Torp T (2006) Tine forces established by a two-level model and the draught requirement of rigid and flexible tines. *Soil & Tillage Research* 90(1-2):230-241.

Chertkiattipol S, Niyamapa T (2010) Variations of torque and specific tillage energy for different rotary blades. *Agricultural Engineering* 19(3):1-14.

Hendrick JG, Gill WR (1978) Rotary blade design parameters, V: Kinematics. *Transactions of the ASAE* 21(4):658-660.

Huang MH, Wang XH, Pang ZY (2013) Research Status and Prospect of *Cyperus esculentus*. *Crop Research* 27(03):293-295+301.

Iwasaki K, Miyabe Y, Kashiwagi S (1992) Tillage resistance on tip and straight portion of a rotary blade. *Memoirs of the Faculty of Agriculture Kagoshima University* 28:143-151.

Jing YY, Xie YY, Qi HY, Xing JZ, Mijiti HA (2014) Preliminary Study on the Introduction and Cultivation of *Cyperus esculentus* in Southern Xinjiang. *Xinjiang Animal Husbandry* (08):29-30.

Koc A, Koparan C, Baig A (2017) Laboratory evaluation of high-frequency vibrations on soil cutting force. In: *Annual International Meeting Spokane*. Washington, ASABE, Proceedings...

Lin SY, Zhang P, Xu L (2016) Research Status and Prospect of rotary blades for Micro-tillers. *Anhui Agricultural Sciences* 44(30):239-240.

Lu ZY, Liu H, Zhang JZ, Ren YF, Cheng YC, Zhang DJ, Shi GF, Cham LR, Zhao XQ (2019) Status quo, problems and suggestions on the development of *Cyperus esculentus* industry. *Modern Agriculture* (06):11+13.

Marenya MO (2009) Performance characteristics of a deep tilling Rotavator. Pretoria, University of Pretoria.

Matin MA, Fielke JM, Desbiolles JMA (2015) Torque and energy characteristics for strip-tillage cultivation when cutting furrows using three designs of rotary blade. *Biosystems Engineering* 129(1):329-340.

Niyamapa T, Salokhe VM (2000) Soil disturbance and force mechanics of vibrating tillage tool. *Journal of Terramechanics* 37(3):151-166.

Rao G, Chaudhary H, Sharma A (2018) Design and analysis of vibratory mechanism for tillage application. *Open Agriculture* 3(1):437-443.

Rao G, Chaudhary H, Sharma A (2019) Optimal design and analysis of oscillatory mechanism for agricultural tillage operation. *SN Applied Sciences* 1(8):19-25.

- Razzaghi E, Sohrabi Y (2016) Vibratory soil cutting a new approach for the mathematical analysis. *Soil&Tillage Research* 159:33-40.
- Salokhe VM, Ramalingam N (2003) Effect of rotation direction of a rotary blade on draft and power requirements in a Bangkok clay soil. *Journal of Terramechanics* 39(4):195-205.
- Shahgoli G, Fieke J, Desbiolles J (2010) Optimising oscillation frequency in oscillatory tillage. *Soil&Tillage Research* 106(2):202-210.
- Shahgoli G, Saunders C, Desbiolles J (2009) The effect of oscillation angle on the performance of oscillatory tillage. *Soil&Tillage Research* 104(1):97-105.
- Soeharson O, Radite PA (2010) Analytical study of self-excited vibration on single degree of freedom vibratory-tillage. *ARN Journal of Engineering and Applied Sciences* 5(6):61-66.
- Wang J, Jiang J, Zhao S (2016) Experimental research on resistance reduction for carrot digging part with self-excited vibration. *Proceedings of ICMECA 2016*.
- Wang YX, Wu SX, Zhou LP, Zhang KH, Li PX (2020a) Research progress on quality analysis and processing and utilization of *Cyperus esculentus*. *Food Industry* 41(10):273-276.
- Wang LR (2020b) Study on Shear Strength of Root-Soil Complexes of Different Plant Communities and Evaluation of Soil Consolidation Effect on Steep Slopes on Loess Plateau. Xianyang, Northwest A&F University.
- Wang RY, Wang XS, Xiang H (2019) A Multipurpose emerging oil crop-*Cyperus esculentus*. *China Oil* 44(1):1-4.
- Wang ZC, Li SS, Liang X, Xu LJ, Zou XL (2022) Development Status and Prospects of *Cyperus esculentus* Industry in China. *Technology and Industry* 22(01):62-67.
- Yan HZ, Kan Y, Liu XH, He BH, Tang H, Qiang JJ (2022) Comprehensive evaluation of shear and anti-scour performance of two kinds of ridge fence root-soil complexes in karst sloping land. *Journal of Ecology* 42(05):1811-1820.
- Yang F, Zhu WX (2020) Current Situation and Prospects of Research on *Cyperus esculentus*. *Grain and Oil* 33(01):4-6.
- Yang RT, Ge RL, Hao XT, Wang ZX, Cui TM (2021) Comparison of mechanical properties of composite shear resistance of different types of soil-*Caragana* root system. *Soil Bulletin* 52(04):821-827.
- Yang ZL (2017) Characteristics and research progress of *Cyperus esculentus*. *Northern Gardening* (17):192-201.
- Zhang B, Liu J, Fan ZX, Guo FD, Hou L, Ma DY, Wang Y (2019) Research progress on the introduction test and green and high-efficiency cultivation technology of *Cyperus esculentus*. *Shandong Agricultural Science* 51(03):147-150.